

# Analysis of the dispersion characteristics in periodic Substrate Integrated Waveguides

A. Coves<sup>a,\*</sup>, A. A. San-Blas<sup>a</sup>, E. Bronchalo<sup>a</sup>

<sup>a</sup>*Departamento de Ingeniería de Comunicaciones-I3E, Universidad Miguel Hernández de Elche, Avenida de la Universidad s/n, E-03202 Elche (Spain)*

---

## Abstract

In this work, we study the dispersion characteristics of the first modes of four periodic structures implemented in Substrate Integrated Waveguide (SIW) technology. Two kind of topologies (based on inductive irises and on rectangular air holes) and two kind of symmetries (normal reflection and glide symmetry) are studied by using electromagnetic simulation software. The obtained results show relevant differences in the characteristics of passbands and stopbands between glide-symmetric and non-glide-symmetric structures. The dispersion characteristics of the first propagating mode are analyzed for finite implementations of all the studied structures. Furthermore, the finite implementations of the structures based on inductive irises have been fabricated and measured, showing good agreement with the simulation results.

*Keywords:* periodic structure, glide symmetry, substrate integrated waveguide (SIW), dispersion, passband, stopband.

---

## 1. Introduction

Periodic media have found many applications in microwave devices associated to the frequency-selective behavior of electromagnetic waves in such media [1, 2, 3]. By properly choosing the geometrical and electrical properties  
5 of the periodic medium, transverse and longitudinal periodic structures can

---

\*Corresponding author  
Email address: [angela.coves@umh.es](mailto:angela.coves@umh.es) (A. Coves)

adapt the electromagnetic properties of waveguides and antennas for specific purposes. Periodicity in the transverse direction of propagation has been used in the last decades in many applications as frequency selective surfaces (FSS) [4], reflect/transmit-arrays [5, 6] or metasurfaces [7, 8]. On the other hand, periodicity in the direction of propagation of the medium comparable to the operation wavelength results in the presence of permitted and forbidden frequency bands [9, 10], which has been widely used in different applications as waveguide filters [11], artificial transmission lines [12], or periodic leaky-wave antennas [13].

In the last two decades, an increasing interest has emerged to describe the dispersion characteristics of wave propagation in periodic structures, both dielectric or metallic, with different frequency-dependent propagation performances. Among them, we can find the frequency stopband feature in electromagnetic band-gap (EBG) structures [14, 15, 16, 17], emergence of propagating, nonpropagating and complex Floquet modes in periodic dielectric-based structures [18, 19], artificial negative refractive index metamaterials (NRIM) [20, 21, 22, 23, 24], or miniaturized slow-wave structures [25].

Recently, higher symmetries (glide and screw symmetries) have been proposed for periodic structures in the form of corrugations for designing lenses [26], to increase the stopbands for use in gap waveguide technology [27, 28], to design band-pass periodic filters in Substrate Integrated Waveguide (SIW) technology based on complementary split-ring resonators [29], and also for increasing the operational bandwidth of mushroom-type EBG structures [30].

The purpose of this work is to analyze the dispersion characteristics of waves propagating in periodic Substrate Integrated Waveguides with different periodic configurations, highlighting the dispersive nature of the propagating modes of the unit cell when approaching the stopbands, and showing the effect of introducing glide symmetry.

The paper is organized as follows. Section 2 describes the unit cells of the different geometries studied in this analysis. In Section 3, the dispersion diagram of the different periodic propagation media is analyzed, and we focus on the dispersive properties of the first propagating mode of the unit cell within the

first passband. In Section 4, we present finite implementations of the different periodic geometries analyzed, and the obtained scattering parameters and group delay of the truncated topologies have been used to check the dispersion behavior of the **fundamental mode** of the different infinitely periodic geometries analyzed. Two prototypes of the periodic structures analyzed have been fabricated and measured for validating purposes. Finally, a summary of our main conclusions is reported in Section 5.

## 2. Geometries of the Periodic Media Considered in the Analysis

Fig. 1 shows the unit cells of the different periodic media that are considered in the analysis. Following the design rules of [31], the vias defining the lateral walls of the analyzed SIW structures have diameter  $d_v = 0.7$  mm and separation  $s_v = 1$  mm (see Fig. 1(a)), which guarantees negligible radiation losses.

The first case under analysis is defined by periodically inserting pairs of symmetrical thick inductive irises inside a SIW (see Fig. 1(a)). The irises are characterized by their thickness  $s_1$  and they are separated a distance  $s_2$  in the x-axis. Besides,  $p$  represents the periodicity in the direction of propagation. The second structure analyzed is obtained by applying a translation of  $p/2$  in the longitudinal direction of one of the irises in each pair (see Fig. 1(b)), resulting in a glide symmetry (i.e., a translation of  $p/2$  and a reflection with respect to the  $w/2$  plane from one iris to the other). The third case under study (see Fig. 1(c)) is defined by periodically removing the dielectric substrate to form pairs of rectangular air holes symmetrically with respect to the  $w/2$  symmetry plane of a SIW, characterized by their width  $t_1$  and separated  $t_2$ . The last case is obtained by a translation in the longitudinal direction of  $p/2$  of one of the rectangular air holes in each pair with respect to the other one (see Fig. 1(d)), resulting again in a glide symmetry. Fig. 2 shows a finite section of the different periodic SIW structures under study.

In order to compare the dispersion characteristics of the structures under analysis, the spatial period has been fixed to  $p = 16$  mm for all cases. In addi-

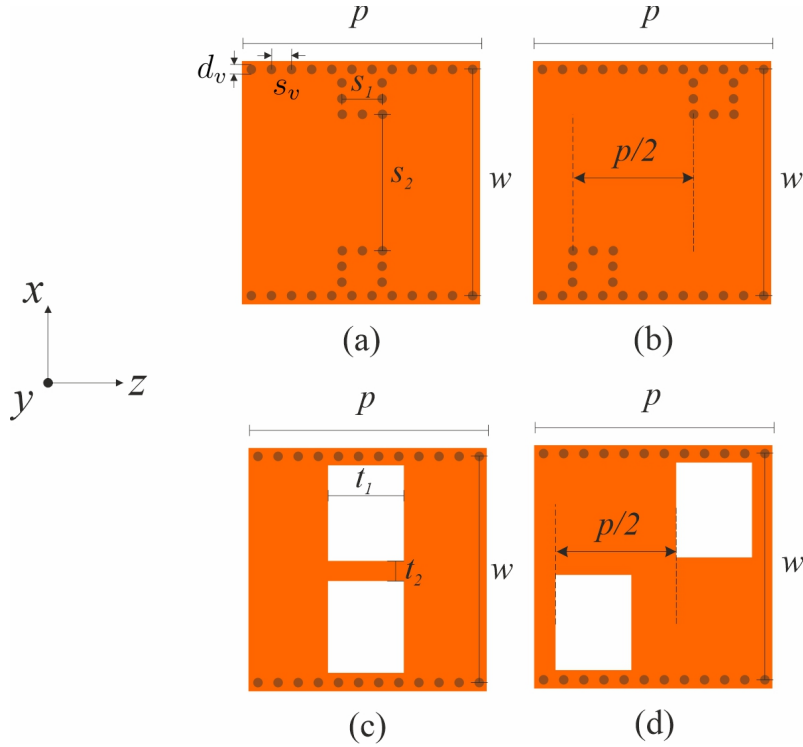


Figure 1: Unit cell of the periodic SIW with the following inserts: (a) two symmetrical thick inductive irises (conventional structure); (b) two thick inductive irises with a translation of  $p/2$  in the longitudinal direction of one of the irises in each pair (glide symmetry); (c) two symmetrical rectangular air holes (conventional structure); (d) rectangular air holes with a translation of  $p/2$  in the longitudinal direction of one of the rectangular air holes in each pair with respect to the other one (glide symmetry).

tion, the parameters of the basis SIW waveguide have been set to the following values: width  $w = 15.8$  mm, height  $b = 0.63$  mm (referred to the  $y$ -axis depicted in Fig. 1) and relative permittivity of the substrate equal to 10. The influence of these parameters, which are directly related to the bandwidth and location of the different permitted and forbidden bands, has been extensively analyzed in the technical literature [1, 32]. It is important to mention that, as a consequence of the linearity of the field equations, the results can be directly scaled to any desired frequency range.

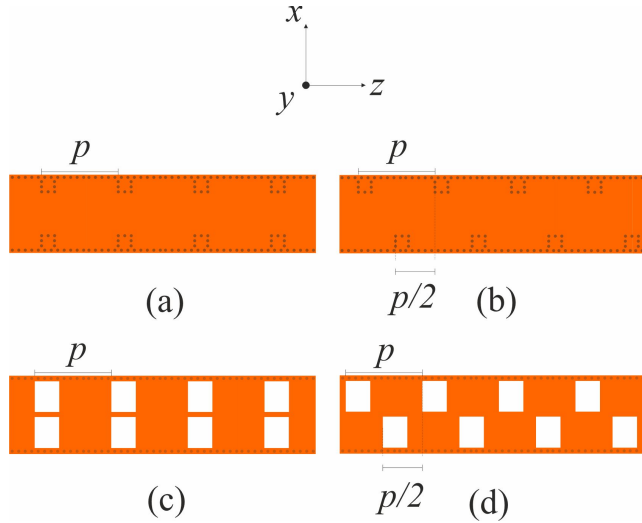


Figure 2: Finite size representations of the periodic structures under study. (a) SIW based on thick inductive irises; (b) SIW based on thick inductive irises with glide symmetry; (c) SIW based on rectangular air holes; (d) SIW based on rectangular air holes glide symmetry.

### 3. Analysis of the dispersion diagrams

75 Simulations of the dispersion diagram of the unit cell of the different periodic media have been carried out using the commercial software Ansys HFSS, which is based on the Finite Element Method [33]. Alternative methodologies for calculating the dispersion diagram of periodic propagation media have been presented in [34, 35, 19, 36].

80 **In all the analyzed cases**, the dispersion diagram of the first two modes of the periodic propagation media (a SIW with periodic inserts along the direction of propagation) has been represented with solid line, using different colours (black for the first mode and blue for the second mode). The dispersion diagram of the same SIW without the periodic inserts is also represented in dashed lines  
85 for comparison. All these guiding media are characterized by the existence of a cutoff frequency below which the fields cannot propagate, and also by a dispersive nature of the field propagation which will be shown next.

The [first](#) case in the study (see Fig. 1(a)) corresponds to a SIW where pairs of symmetric thick inductive irises of thickness  $s_1 = 2.85$  mm and separated a distance  $s_2 = 9.9$  mm in the x-axis have been periodically inserted. Fig. 3 shows the dispersion diagram of the first two modes (solid lines). It can be seen that the normalized cutoff frequency of the first mode ( $\omega_c p/c = 1.23$ ) has increased with respect to that of the uniform SIW ( $\omega_c p/c = 1.04$ ), because, somehow, we have a lower mean width of the SIW in this case. Additionally, a first stopband appears between  $[1.45 - 1.70]\omega p/c$ . Thus, a first passband is defined between the cutoff frequency of the fundamental mode and the lowest edge of the first stopband. This fact makes this periodic structure suitable for filtering applications, where the period can be properly selected for adjusting the upper limit of the passband and the bandwidth of the rejection band. However, it can be checked in Fig. 3 that the fundamental mode becomes more dispersive in the vicinity of the stopband, i.e., the curve flattens as it approaches the  $\beta_z p = \pi$  line. This [behavior](#), added to the fact that the mode is also highly dispersive near the cutoff frequency, could make it difficult to use this topology as a filtering structure, since, in a practical implementation, the frequency range within the passband with acceptable group delay flatness will be very reduced.

Concerning the analysis of the [glide-symmetric](#) cases in Fig. 1, we start with the structure represented in Fig. 1(b), i.e., a SIW periodically loaded with thick inductive irises of thickness  $s_1$  and separated a distance  $s_2$  in the x-axis, but with glide symmetry, which is obtained from the previous case by applying a translation in the longitudinal direction of  $p/2$  of one of the irises in each pair with respect to the other one. Fig. 4 shows the dispersion diagram of the first two modes of the iris-loaded [glide-symmetric](#) case. Comparing the results in this figure with those of Fig. 3, it can be checked that the cutoff frequency of the first mode has not been modified by the [glide symmetry](#) operation. However, the most important difference is that, in the [glide-symmetric](#) configuration, the previously observed stopband of the first propagation mode has disappeared, as previously observed in other [glide-symmetric](#) structures [27, 36], and thus the curve of the first mode becomes almost straight over a wide range of frequencies. Then,

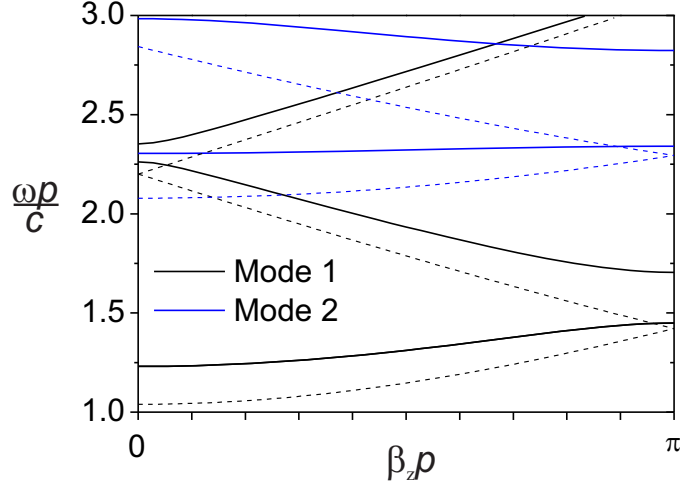


Figure 3: Dispersion diagram of the first two modes of the periodic structure depicted in Fig. 1(a), consisting of a SIW periodically loaded with pairs of symmetric thick inductive irises of thickness  $s_1 = 2.85$  mm, and separated a distance  $s_2 = 9.9$  mm in the x-axis. The dispersion diagram of the uniform SIW is also represented in dashed lines for comparison.

two interesting consequences are derived by the glide-symmetric operation: a  
 120 substantial increase of the first passband, and an essentially non-dispersive be-  
 havior in a much wider band. This fact, already reported in [37, 38, 39, 40],  
 is one of the most relevant features of glide-symmetric structures and is likely  
 to find interesting applications in the near future. Thus, this glide-symmetric  
 structure is more suitable for filtering applications, where the passband on one  
 125 hand, and the frequency range with nearly flat group delay, on the other hand,  
 have been substantially increased.

Note that there is a very narrow stopband of the first mode at the  $\beta_z p = 0$   
 edge at higher frequencies for this particular configuration. This stopband could  
 be widened by properly modifying the structure parameters. For instance, Fig. 5  
 130 shows how the width of the stopband can be directly increased by reducing the

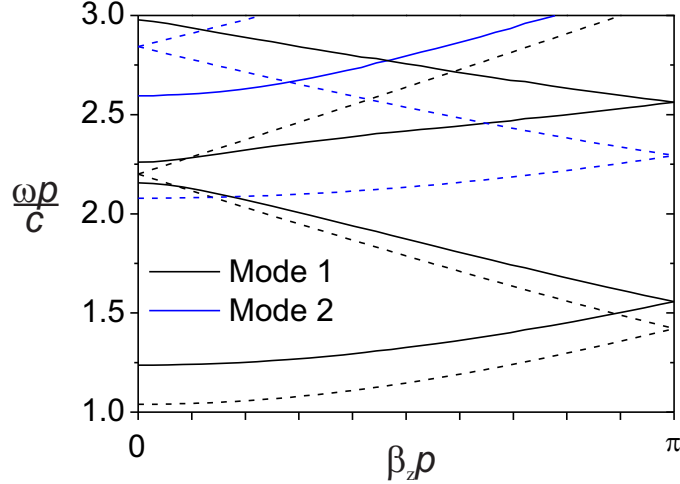


Figure 4: Dispersion diagram of the periodic structure depicted in Fig. 1(b), i.e., the glide-symmetric configuration obtained from the component in Fig. 1(a), resulting in a translation of  $p/2$  and a reflection with respect to the  $w/2$  plane from one iris to the next one. The dispersion diagram of the uniform SIW is also represented in dashed lines for comparison.

$s_2$  parameter, although this leads to a reduction in the passband. However, a very wide stopband can also be found in other type of glide-symmetric SIW structures [29].

The third case in the study (see the unit cell depicted in Fig. 1(c)) is defined  
 135 by periodically etching pairs of rectangular air holes symmetrically with respect  
 to the  $w/2$  plane of the SIW, characterized by their width  $t_1$  and separated  
 $t_2$ , whose periodic nature again provides a stopband in the dispersion diagram.  
 The dimensions of the rectangles have been properly chosen for obtaining a first  
 passband similar to that obtained in the structure in Fig. 1(a), being  $t_1 = 5.46$   
 140 mm and  $t_2 = 0.6$  mm. Fig. 6 shows the dispersion diagram of the first two  
 modes of this periodic propagation medium (solid lines). The normalized cutoff  
 frequency of the first mode ( $\omega_cp/c = 1.175$ ) has increased with respect to that



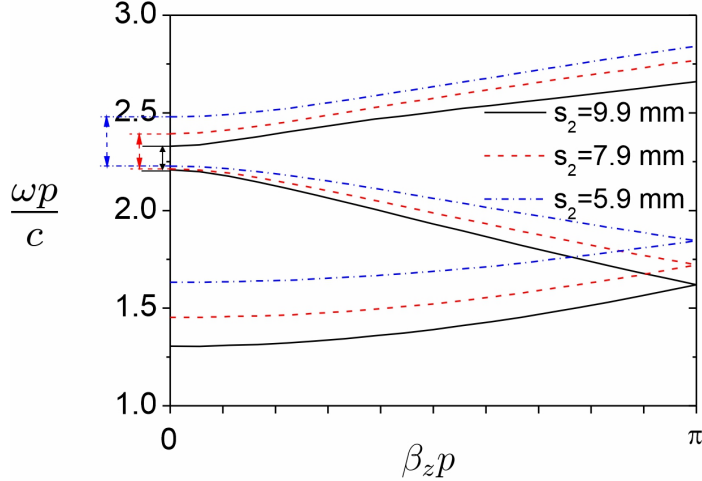


Figure 5: Effect of the variation of the parameter  $s_2$  on the dispersion diagram of the periodic structure depicted in Fig. 1(b).

of the uniform SIW ( $\omega_c p/c = 1.04$ ), because the mean relative permittivity of the dielectric is lower in this case. Additionally, the stopband, which falls  
 145 between  $[1.45 - 1.84]\omega p/c$ , is wider in this case, although the first passband of the structure, defined between the cutoff frequency of the fundamental mode and the lowest edge of the first stopband, is very similar to that obtained in the structure analyzed in Fig. 1(a). This periodic structure may also be suitable for filtering applications, being the period a design parameter for adjusting the passband and the rejection band. However, as in the previous periodic cases,  
 150 the highly dispersive character of the fundamental mode at the passband edges will result in poor performance as a filtering structure in terms of group delay.

The last case to be analyzed is obtained by applying a glide-symmetric operation of the unit cell in Fig.1(c), with a translation of  $p/2$  and a reflection with respect to the  $w/2$  plane from one rectangular air hole to the next one  
 155 (see Fig. 1(d)). Fig. 7 shows the dispersion diagram of the first two modes of this glide-symmetric structure. Comparing these results with those represented in Fig. 6, again, it can be checked that applying glide symmetry leaves the cutoff

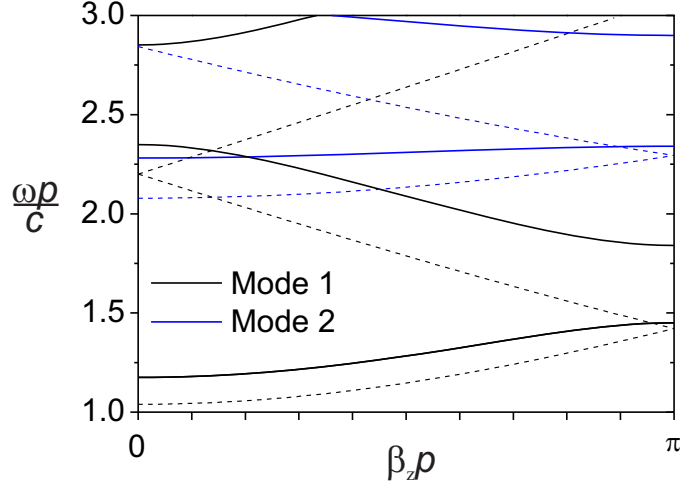


Figure 6: Dispersion diagram of the first two modes of the periodic structure depicted in Fig. 1(c), consisting of a SIW where pairs of rectangular holes with parameters  $t_1 = 5.46$  mm and  $t_2 = 0.6$  mm have been periodically etched symmetrically with respect to the  $w/2$  plane. The dispersion diagram of the uniform SIW is also represented in dashed lines for comparison.

frequency of the first mode unchanged, and most importantly, that the stopband  
 160 of the first propagation mode disappears, as already observed in the structure  
 analyzed in Fig. 1(b), so the dispersion curve of the first mode becomes al-  
 most straight over a wide range of frequencies. As a consequence, a substantial  
 increase of the first passband, and an essentially non-dispersive behavior in a  
 much wider band has been achieved. Besides, a stopband of the first mode at  
 165 higher frequencies can be observed, which may be widened by a proper selection  
 of the rectangular air holes parameters for filtering applications [19]. Thus, this  
 glide-symmetric structure is more suitable for wideband filtering applications,  
 where the passband on one hand, and the frequency range with flat group delay  
 on the other hand, have been greatly increased.

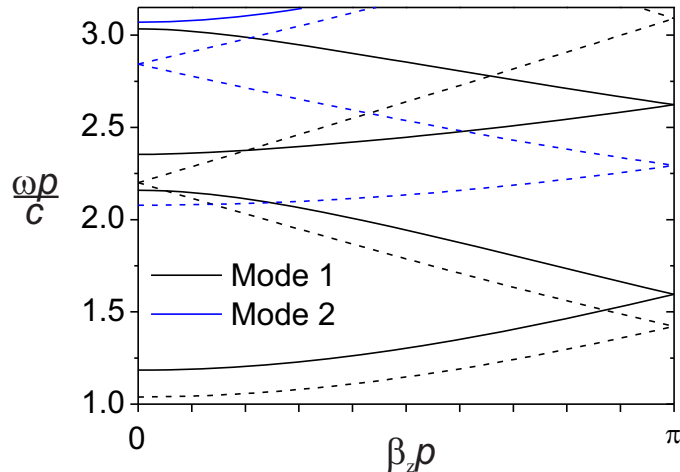


Figure 7: Dispersion diagram of the first two modes of the periodic structure of Fig. 1(d), i.e., by applying a glide-symmetric operation to the unit cell in Fig. 1(c), resulting in a translation of  $p/2$  and a reflection with respect to the  $w/2$  plane from one rectangular air hole to the next one. The dispersion diagram of the uniform SIW is also represented in dashed lines for comparison.

#### 170 4. Finite Implementation of the Periodic Structures and Experimental Validation

In order to check the dispersion characteristics of the analyzed EBG structures studied in Section 3, we have analyzed finite implementations of such periodic propagation media, and the frequency behavior of their scattering parameters and group delay have been obtained. A sufficiently high number of periodic cells in the finite periodic structures has been chosen in order to achieve a deep enough rejection band corresponding to the first stopband of the infinite periodic structures. On the other hand, truncation of the infinite periodic propagation media also degrades the passband performances of the obtained electrical responses, due to the mismatch between the impedance of the propagating mode in the periodic media and the impedance of the access ports [41]

which may result in unacceptable return loss levels, and could degrade the group delay flatness. To overcome this problem, input and output tapered transitions from microstrip to SIW [42] have been designed and added to the truncated  
185 periodic SIW structures.

It is worth mentioning that in this periodic approach, differently from a classical filter synthesis approach, a final optimization process must always be performed related to the taper transitions from microstrip to SIW, with the aim of obtaining certain prescribed return losses, which has led to the design of  
190 the electrical responses of the different structures investigated in this work. In this final optimization process, we used the Quasi Newton (Gradient) Optimizer provided by Ansys HFSS commercial software. The optimized variables were the width and length of the taper, and we selected as cost function a  $S_{11}$  (dB) lower than  $-15$  dB in the pass-band.

195 The simulated electrical response (scattering parameters and group delay) of finite implementations of the periodic and glide-symmetric SIW structures (see Fig. 2) are shown next. Dielectric and conductor losses have been considered in all simulations ( $\tan \delta = 0.0035$  for the substrate material and  $\sigma_{Cu} = 5.8 \cdot 10^7 \text{ S} \cdot \text{m}^{-1}$  for the metallization). Additionally, two prototypes corresponding  
200 to the iris-loaded periodic and glide-symmetric cases (structures represented in Fig.2(a) and (b)) have been manufactured and measured for validation purposes. In the following, the same parameters defined in Section 3 for the periodic inserts (irises/rectangular air holes) and the periodicity have been used.

Fig. 8 shows the scheme of the finite periodic structure with the same unit  
205 cell of Fig. 1(a), and whose dispersion diagram was analyzed in Fig. 3, with 6 periodic cells, i.e., 6 pairs of thick inductive irises. Fig. 9(a) represents the simulated and measured scattering parameters of the structure (left axis), along with the dispersion curve of the first mode of the infinite periodic structure in the passband (red line, right axis), while the group delay is represented in Fig. 9(b).  
210 In Fig. 9(a), the  $S_{21}$  parameter of the original SIW is also represented in blue line for comparison purposes.

Although this structure may be used as a bandpass filter at the sight of the

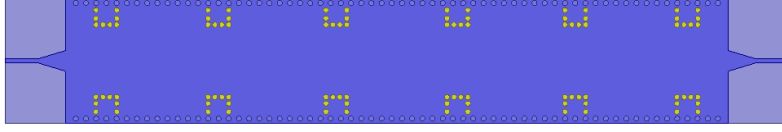


Figure 8: Scheme of a finite periodic structure with the same unit cell represented in Fig. 1(a), with 6 periodic cells, i.e., 6 pairs of thick inductive irises.

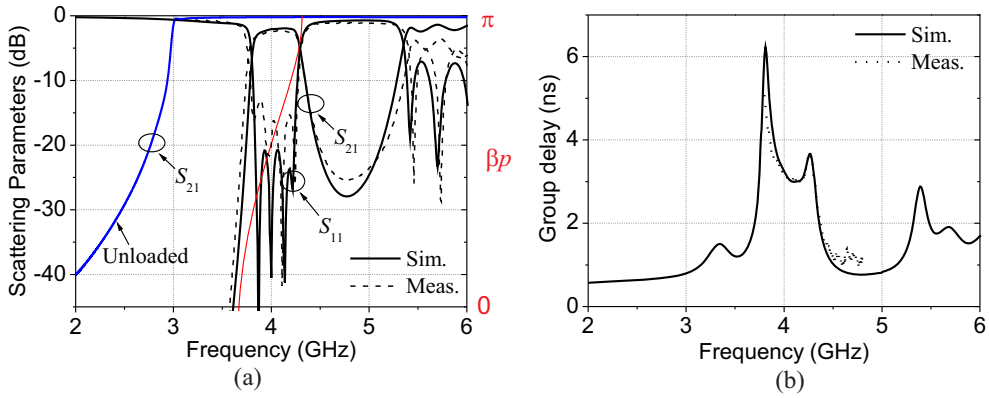


Figure 9: Simulated and measured frequency response of the finite periodic structure of Fig. 8. (a) Scattering parameters (left axis) and dispersion diagram of the first mode of the structure in the pass-band (red line, right axis). (b) Group delay.

scattering parameters in Fig. 9(a), Fig. 9(b) reveals that an acceptable group delay flatness in the passband is not achieved. Besides, a good response in terms of return losses ( $RL_{min} = 22$  dB) has been obtained in this case.

Next, a finite implementation of the same periodic structure but with glide symmetry (see the corresponding unit cell in Fig. 1(b)) has been designed, whose scheme is represented in Fig. 10. The simulated and measured scattering parameters and group delay of this glide-symmetric structure are represented in Fig. 11. The  $S_{21}$  parameter of the original SIW is also plotted (blue line) for comparison.

In Fig. 11(a), the dispersion diagram of the first mode of the structure has been represented (red line, right axis) for comparison, which is in accordance

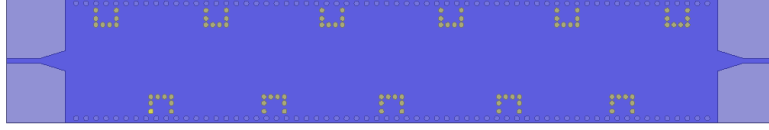


Figure 10: Scheme of a finite **glide-symmetric** structure with the unit cell represented in Fig. 1(b), with 5 and a half periodic cells.

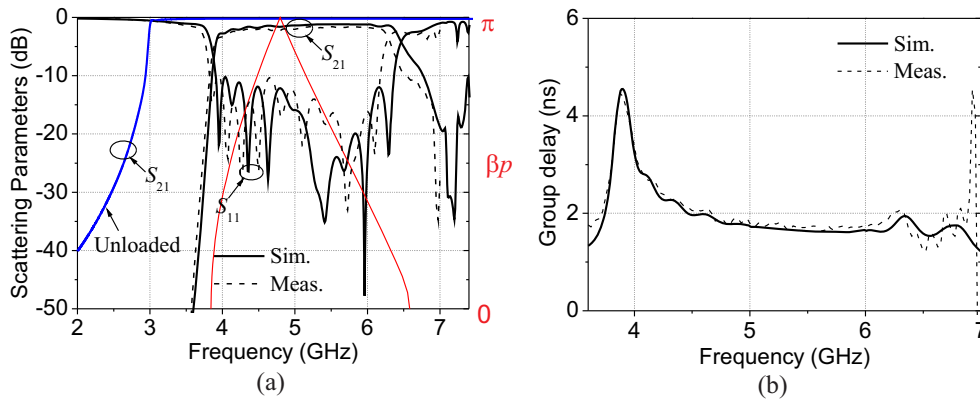


Figure 11: Simulated frequency response of the finite **glide-symmetric** structure shown in Fig. 10. (a) Scattering parameters (left axis) and dispersion diagram of the **first mode** of the structure in the pass-band (red line, right axis). (b) Group delay.

with the scattering parameters (left axis). As pointed out in Section 3, it can  
 225 be checked that there is a considerable increase of the passband in this **glide-symmetric** configuration, with  $RL_{min} = 11$  dB. In this figure, it can also be checked that the spurious free band is not good, as it was pointed out when describing its dispersion diagram, which showed a quite narrow stopband for this particular configuration. However, a most interesting result can be seen in  
 230 Fig. 11(b), which reveals that the obtained group delay in the passband is nearly flat in a very wide band in this case, making this structure an ideal candidate for wideband filtering applications.

Finally, we have also designed finite implementations of the periodic and **glide-symmetric** structures represented in Fig. 1(c) and Fig. 1(d), i.e, with rect-

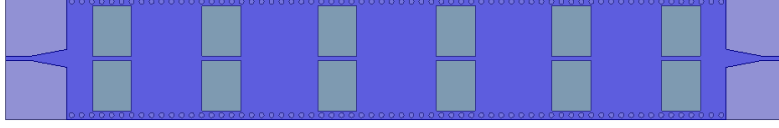


Figure 12: Scheme of a finite periodic structure with the same unit cell represented in Fig. 1(c), with six pairs of rectangular air holes etched symmetrically with respect to the  $w/2$  plane of the SIW.

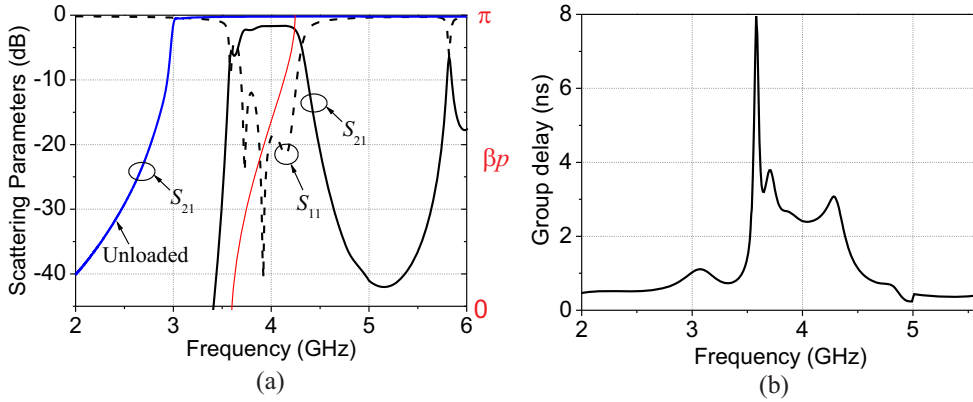


Figure 13: Simulated frequency response of the finite periodic structure of Fig. 12. (a) Scattering parameters (left axis) and dispersion diagram of the **first mode** of the structure in the pass-band (red line, right axis). (b) Group delay.

235 angular air holes periodically etched along the structure. Fig. 12 shows the  
 scheme of the finite implementation of the unit cell depicted in Fig. 1(c) (whose  
 dispersion diagram was analyzed in Fig. 6), with 6 periodic cells, i.e., six pairs of  
 rectangular air holes etched symmetrically with respect to the  $w/2$  plane of the  
 SIW. Fig. 13(a) represents the simulated scattering parameters of the structure  
 240 (left axis), along with the dispersion curve of the **first mode** of the infinite peri-  
 odic structure in the passband (red line, right axis), while the simulated group  
 delay is represented in Fig. 13(b). The  $S_{21}$  parameter of the original SIW is  
 also plotted (blue line) for comparison.

In this case, although a good matching has not been achieved at the lower

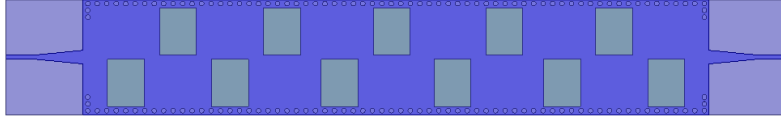


Figure 14: Scheme of a finite **glide-symmetric** structure with the same unit cell represented in Fig. 1(d), with 5 and a half periodic cells.

245 end of the passband, it can be seen that a good response in terms of insertion losses (lower than 2 dB) and return losses (higher than 12 dB) has been achieved, as it can be observed in the scattering parameters represented in Fig. 13(a). A sharp variation of the group delay is observed in Fig. 13(b) around 3.55 GHz, associated to the mentioned mismatch, which may be avoided by tapering the  
 250 periodic structure so as to provide a gradual change from the unloaded SIW to the final periodically loaded structure. However, as explained in Section 3, the dispersive character of the **propagative mode** at both ends of the passband will still derive in a non-flat group delay, which makes this structure unsuitable for wideband filtering applications.

255 A finite implementation of the same periodic structure but with glide symmetry (see the unit cell in Fig. 1(d)) has been designed, whose scheme is represented in Fig. 14. The simulated scattering parameters (black line, left axis) along with the dispersion diagram of the **first mode** of the **glide-symmetric** structure (red line, right axis) are shown in Fig. 15(a), while the calculated group delay is  
 260 represented in Fig. 15(b). The  $S_{21}$  parameter of the original SIW is also plotted (blue line) for comparison.

Again, in Fig. 15(a) it can be checked that there is a considerable increase of the passband when applying the **glide-symmetric** operation, although keeping the total length of the structure unchanged. **In this case, the same mismatch**  
 265 **can be observed at both ends of the passband ( $RL_{min} = 7$  dB at 3.7 GHz, while  $RL_{min} = 6$  dB at 6.3 GHz).** Regarding the group delay of the structure represented in Fig. 15(b), in spite of the sharp variation of the group delay around the beginning of the passband, we can see that the obtained group



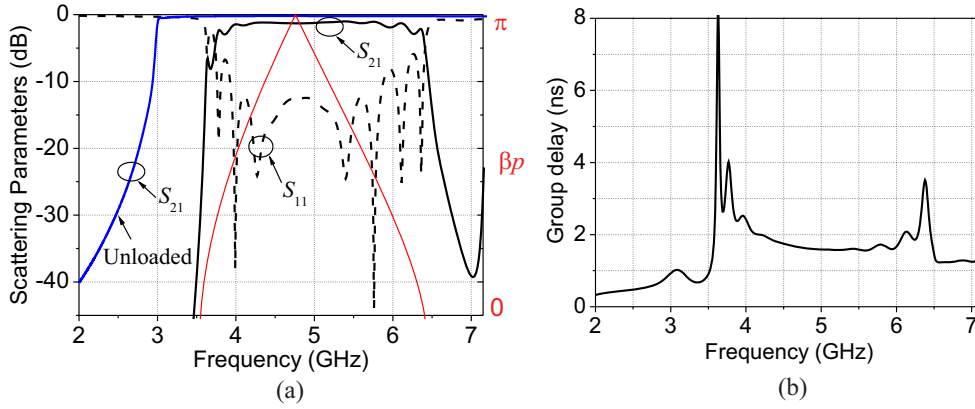


Figure 15: Simulated frequency response of the finite glide-symmetric structure shown in Fig. 14.(a) Scattering parameters (left axis) and dispersion diagram of the first mode of the structure in the pass-band (red line, right axis). (b) Group delay.

delay in the passband is nearly flat in a very wide band, making this structure  
 270 much more suitable for wideband filtering applications.

It is worth noting that the improvement of the flatness of the group delay  
 observed in the analyzed glide-symmetric structures is due to the large passband  
 implemented in these responses and, therefore, it cannot be considered as a  
 feature inherent to the glide-symmetric configuration. Authors would like to  
 275 recall that, in order to further improve the flatness of the group-delay responses,  
 complex transmission zeros would need to be realized [43]. The in-line topology  
 used in the filtering structures designed in this work, however, does not allow  
 for the implementation of transmission zeros.

## 5. Conclusion

280 The dispersion characteristics of the first modes of different periodic SIW  
 structures with periodicity in the direction of propagation have been studied.  
 The analysis of the dispersion diagram of the infinitely periodic structures has  
 revealed, as expected, the existence of alternated passbands and stopbands in all

the proposed periodic structures, making them suitable for filtering applications.  
285 However, a detailed analysis of the dispersion properties of the **first propagating mode** in the different periodic topologies analyzed has revealed that the application of a **glide-symmetric** operation to their original periodic counterparts can enhance the passband bandwidth of the **first propagative mode**, while keeping a nearly linear dependence of its dispersion curve with frequency in such pass-  
290 band. In order to have evidence of such results, finite implementations of the periodic structures have been designed and analyzed, whose scattering parameters and group delay have revealed less dispersive configurations at the same time as a much wider passband when using glide symmetry.

## Funding

295 This research was supported by the Ministerio de Ciencia e Innovación, Spanish Government, under R&D Project PID2019-103982RB-C43.

## References

- [1] R. E. Collin, *Field Theory of Guided Waves*, IEEE Press, 1991.
- [2] D. M. Pozar, *Microwave Engineering*, Wiley, 3rd ed., 2005.
- 300 [3] F. Yang, Y. Rahmat-Samii, *Electromagnetic Band Gap Structures in Antenna Engineering*, Cambridge University Press, 2009.
- [4] B. Munk, *Frequency Selective Surfaces: Theory and Design*, John Wiley and Sons, 2000.
- [5] J. Huang, J. Encinar, *Reflectarray antennas*, Wiley, Inter Science, 2000.
- 305 [6] N. Gagnon, A. Petosa, D. A. McNamara, Research and development on phase-shifting surfaces (PSSs), *IEEE Transactions on Antennas and Propagation* 55 (2013) 29–48.
- [7] E. Martini, S. Maci, *Transformation Electromagnetics and Metamaterials*, Springer, 2000, pp. 83–116.

- 310 [8] V. G. Ataloglou, M. Chen, M. Kim, G. V. Eleftheriades, Microwave huygens' metasurfaces: Fundamentals and applications, *IEEE Journal of Microwaves* 1 (2021) 374–388.
- [9] L. Brillouin, *Wave Propagation in Periodic Structures. Electric Filters and Crystal Lattices*, McGraw-Hill, 1953.
- 315 [10] C. Kittel, *Introduction to Solid State Physics*, Wiley, 1995.
- [11] R. J. Cameron, C. M. Kudsia, R. R. Mansour, *Microwave Filters for Communication Systems*, Wiley, 2007.
- [12] F. Martin, *Artificial Transmission Lines for RF and Microwave Applications*, John Wiley & Sons, Ltd, 2015.
- 320 [13] D. R. Jackson, A. A. Oliner, *Leaky-wave antennas*, John Wiley and Sons, 2007, pp. 325–367.
- [14] F. R. Yang, R. Coccioli, Y. Qian, T. Itoh, Planar PBG structures: basic properties and applications, *IEICE Transactions on Electronics E83-C* (2000) 687–696.
- 325 [15] A. A. Oliner, Periodic structures and photonic-band-gap terminology: historical perspective, in: *2013 IEEE MTT-S International Microwave Symposium Digest (MTT)*, 1999, pp. 295–298.
- [16] P. S. Kildal, A. U. Zaman, E. Rajo-Iglesias, E. Alfonso, A. Valero-Nogueira, Design and experimental verification of ridge gap waveguide in bed of nails for parallel-plate mode suppression, *IET Microwaves, Antennas and Propagation* 5 (2011) 262–270.
- 330 [17] M. Bozzi, L. Germani, S. Minelli, L. Perregrini, P. de Maagt, Efficient calculation of the dispersion diagram of planar electromagnetic band-gap structures by the MoM/BI-RME method, *IEEE Transactions on Antennas and Propagation* 53 (2005) 29–35.
- 335

- [18] S. Simsek, E. Topuz, Some properties of generalized scattering matrix representations for metallic waveguides with periodic dielectric loading, *IEEE Transactions on Microwave Theory and Techniques* 55 (2007) 2336–2344.
- [19] A. Coves, S. Marini, B. Gimeno, V. Boria, Full-wave analysis of periodic dielectric frequency-selective surfaces under plane wave excitation, *IEEE Transactions on Antennas and Propagation* 60 (2012) 2760–2769.
- [20] C. Y. Cheng, R. W. Ziolkowski, Tailoring double-negative metamaterial responses to achieve anomalous propagation effects along microstrip transmission lines, *IEEE Transactions on Microwave Theory and Techniques* 51 (2003) 2306–2314.
- [21] R. S. Kshetrimayum, L. Zhu, Guided-wave characteristics of waveguide based periodic structures loaded with various fss strip layers, *IEEE Transactions on Microwave Theory and Techniques* 53 (2005) 120–124.
- [22] R. W. Ziolkowski, N. Engheta, Metamaterial special issue introduction, *IEEE Transactions on Antennas and Propagation* 51 (2003) 2546–2549.
- [23] B. Li, C. Yang, J. Shi, J. Li, A. Zhang, Circularly polarized array with enhanced isolation using magnetic metamaterials, *Electronics* 8 (2019) 1356.
- [24] K. W. Eccleston, I. G. Platt, Identifying near-perfect tunneling in discrete metamaterial loaded waveguides, *Electronics* 8 (2019) 84.
- [25] C. Zhou, H. Y. D. Yang, Design considerations of miniaturized least dispersive periodic slow-wave structures, *IEEE Transactions on Microwave Theory and Techniques* 56 (2008) 467–474.
- [26] O. Quevedo-Teruel, J. Miao, M. Mattsson, A. Algaba-Brazalez, M. Johansson, L. Manholm, Glide-symmetric fully metallic luneburg lens for 5G communications at ka-band, *IEEE Antennas and Wireless Propagation Letters* 17 (2018) 1588–1592.

- [27] N. Memeletzoglou, C. Sanchez-Cabello, F. Pizarro-Torres, E. Rajo-Iglesias, Analysis of periodic structures made of pins inside a parallel plate waveguide, *IEEE Antennas and Wireless Propagation Letters* 11 (2019) 582.
- 365 [28] M. Ebrahimpouri, O. Quevedo-Teruel, E. Rajo-Iglesias, Design guidelines for gap waveguide technology based on glide-symmetric holey structures, *IEEE Microwave and Wireless Components Letters* 27 (6) (2017) 542–544.
- [29] J. Martínez, A. Coves, F. Mesa, O. Quevedo-Teruel, Passband broadening of sub-wavelength resonator-based glide-symmetric SIW filters, *AEU - International Journal of Electronics and Communications* 125 (2020) 153362.
- 370 [30] B. A. Mouris, A. Fernández-Prieto, R. Thobaben, J. Martel, F. Mesa, O. Quevedo-Teruel, On the Increment of the Bandwidth of Mushroom-Type EBG Structures With Glide Symmetry, *IEEE Transactions on Microwave Theory and Techniques* 68 (4) (2020) 1365–1375.
- 375 [31] D. Deslandes, K. Wu, Accurate modeling, wave mechanisms, and design considerations of a substrate integrated waveguide, *IEEE Transactions on Microwave Theory and Techniques* 54 (6) (2006) 2516–2526.
- [32] J. D. Joannopoulos, R. D. Meade, J. N. Winn, *Photonic Crystals*, Princeton University Press, 1995.
- 380 [33] ANSYS, High frequency structure simulator (HFSS).  
URL <https://www.ansys.com>
- [34] F. Bongard, J. Perruisseau-Carrier, J. R. Mosig, Enhanced periodic structure analysis based on a multiconductor transmission line model and application to metamaterials, *IEEE Transactions on Microwave Theory and Techniques* 57 (2009) 2715–2726.
- 385 [35] S. Marini, A. Coves, V. Boria, B. Gimeno, Efficient modal analysis of periodic structures loaded with arbitrarily shaped waveguides, *IEEE Transactions on Microwave Theory and Techniques* 58 (2009) 529–536.

- [36] F. Mesa, R. Rodriguez-Berral, F. Medina, On the computation of the dispersion diagram of symmetric one-dimensionally periodic structures, *Symmetry* 10 (2018) 307.
- [37] M. Ebrahimpouri, O. Quevedo-Teruel, E. Rajo-Iglesias, Ultra-wideband metasurface lenses based on off-shifted opposite layers, *IEEE Antennas and Wireless Propagation Letters* 15 (2016) 484–487.
- [38] G. Valerio, Z. Sipus, A. Grbic, O. Quevedo-Teruel, Accurate equivalent-circuit descriptions of thin glide-symmetric corrugated metasurfaces, *IEEE Transactions on Antennas and Propagation* 65 (2017) 2695–2700.
- [39] O. Dahlberg, R. Mitchell-Thomas, O. Quevedo-Teruel, Reducing the dispersion of periodic structures with twist and polar glide symmetries, *Scientific Reports* 7 (2017) 10136.
- [40] M. Ebrahimpouri, E. Rajo-Iglesias, Z. Sipus, O. Quevedo-Teruel, Cost-effective gap waveguide technology based on glide-symmetric holey EBG structures, *IEEE Transactions on Microwave Theory and Techniques* 6 (2018) 927–934.
- [41] S. Marini, P. Soto, A. Coves, B. Gimeno, V. Boria, Practical design of filters using EBG waveguides periodically loaded with metal ridges, *Progress In Electromagnetics Research C* 63 (2016) 13–21.
- [42] D. Deslandes, K. Wu, Integrated microstrip and rectangular waveguide in planar form, *IEEE Microwave and Wireless Components Letters* 11 (2001) 68–70.
- [43] J.D. Rhodes, [A Low-Pass Prototype Network for Microwave Linear Phase Filters](#), *IEEE Transactions on Microwave Theory and Techniques* 18 (6) (1970) 290–301.